An implicit non-linear numerical scheme for illumination-robust variational optical flow

Sándor Fazekas[1]
fazekas@vision.sztaki.hu
Dmitry Chetverikov[1]
csetverikov@sztaki.hu
József Molnár[2]
molnarj@cdata.hu

[1] Computer and Automation Research Institute
Budapest, Hungary

[2] Eötvös Loránd University
Budapest, Hungary

Abstract

We present an optical flow calculation method based on the variational approach. The method uses an implicit non-linear numerical scheme that makes no assumption on the analytical form of the optical constraints and combines local and global smoothness criteria in a natural way. Defining the optical constraints with normalised cross-correlation, we obtain a technique that is robust against illumination changes in colour and greyscale images.

1 Introduction

Optical flow describes the apparent motion observed in a sequence of images. This, in a natural way, characterises the motion with a displacement field. (See Fig. 1.) The optical flow concept arose from studies of biological visual systems [6]. Several examples can be presented to emphasise the importance of motion in visual sensing. Studies of visual perception [5] revealed that humans use motion directly in recognising aspects of their environment. Insects are essentially blind to anything that is standing still and the camouflage strategies of some animals are effective only as long as they are not moving.

The observation that motion adds relevant information to visual patterns explains the persisting effort in computer vision and related research areas to improve motion analysis and optical flow estimation methods. This has a wide range of applications in fields such as object tracking, robotics, human-machine interaction, driver assistance systems, as well as video compression, super-resolution, and dynamic texture analysis. The main challenge of any vision system lies in integrating local motion information into a coherent global interpretation.

The most widespread approach to define and calculate an optical flow is the use of the *brightness constancy assumption* which assumes that the brightness of a small, moving image region is constant. However, this holds only for Lambertian surfaces at constant illumination conditions. Optical constraints on their own, even if illumination changes are taken into account, are usually insufficient for computing a flow without ambiguity unless the motion estimation is extended to larger regions [8].

BMVC 2009 doi:10.5244/C.23.46

Figure 1: Colour-encoded ground-truth optical flow of the `street` sequence [11].

This problem known as the *aperture problem* [18] is usually solved by introducing *smoothness constraints* on the flow field. Based on the type of employed smoothness constraints, there are two major groups of methods [3]: (1) methods applying *global* and (2) methods using *local* smoothness constraints. The first group includes the variational methods, derived from the Horn-Schunck method [9]. The methods of the second group are usually based on the block matching and the structure tensor schemes, which can be traced back to the Lucas-Kanade approach [10].

In this article, we present a novel numerical scheme for variational optical flow calculation that makes no assumption on the analytical form of the employed optical flow constraint. The scheme works with different smoothness criteria combining local and global methods in a natural way. We use this framework to formulate an illumination-robust optical flow calculation method based on normalised mean-shifted cross-correlation.

2 Variational optical flow calculation

Among numerous techniques used for motion estimation, the variational optical flow calculation methods are currently the most accurate. The variational problem for optical flow calculation is usually formulated as finding the displacement function $\mathbf{u}(\mathbf{x})$ that minimises a functional of the form

$$\mathscr{F}(\mathbf{u}) = \int_{\mathbf{x}} \big(E(\mathbf{x},\mathbf{u}) + \lambda S(\nabla_{\mathbf{x}} \otimes \mathbf{u})\big), \tag{1}$$

where $E(\mathbf{x},\mathbf{u})$, $\mathbf{x} = (x,y)$, $\mathbf{u} = (u,v)$, is a function describing optical constraints, S a function of the derivatives u_α, v_β accounting for the smoothness of the flow. $\otimes$ denotes the dyadic (outer) product of two vectors, while λ is a parameter. Here and in what follows $\alpha,\beta \in \{x,y\}$.

The solution of Eq. (1) is given by the Euler-Lagrange equations

$$E_u - \lambda\left(S_{xu_x} + S_{yu_y}\right) = 0,$$
$$E_v - \lambda\left(S_{xv_x} + S_{yv_y}\right) = 0.$$

Notice that we have a set of two coupled partial differential equations. To find the optical flow $\mathbf{u}$, these are solved numerically.

For simplicity, we assume that

$$S = \frac{1}{2}\left(|\nabla_{\mathbf{x}} u|^2 + |\nabla_{\mathbf{x}} v|^2\right) = \frac{1}{2}\sum_{\alpha}\left(u_\alpha^2 + v_\alpha^2\right). \tag{2}$$

Then from the Euler-Lagrange equations we have, in vector notation,

$$\nabla_{\mathbf{u}} E - \lambda \Delta \mathbf{u} = 0, \tag{3}$$

where the Laplacian Δ is applied to each component of $\mathbf{u}$.

Most of the methods use an iterative solver that improves the optical flow estimate obtained in a previous step as $\mathbf{u} \to \mathbf{u}'$, repeating the procedure until a steady state is reached.

The Laplacian of the optical flow in $\mathbf{u}'$ is usually discretised as

$$\Delta\mathbf{u} \approx \bar{\mathbf{u}} - 4\mathbf{u}', \tag{4}$$

where $\bar{\mathbf{u}}(x,y) = \mathbf{u}(x-1,y) + \mathbf{u}(x,y-1) + \mathbf{u}(x+1,y) + \mathbf{u}(x,y+1)$ is the central sum calculated from the current optical flow estimate $\mathbf{u}$.

For finding $\mathbf{u}'$, at each image point $\mathbf{x}$ we have to solve the two-dimensional root-finding problem

$$\mathbf{g}' - \lambda(\bar{\mathbf{u}} - 4\mathbf{u}') = 0, \tag{5}$$

where $\mathbf{g}'$ is $\nabla_{\mathbf{u}} E$ computed in $\mathbf{u}'$. Observe that $\mathbf{g}'$ is not necessarily linear. However, we can choose E such that it becomes linear.

Horn and Schunck [9] proposed

$$E_{\mathrm{HS}} = \frac{1}{2}\left(I_t + uI_x + vI_y\right)^2 = \frac{1}{2}\left(I_t + \mathbf{u}\nabla_{\mathbf{x}} I\right)^2, \tag{6}$$

where $I(\mathbf{x},t)$ is the image brightness. The equation $I_t + \mathbf{u}\nabla_{\mathbf{x}} I = 0$ is a first-order Taylor approximation of brightness constancy between two consecutive images in a sequence, $I(\mathbf{x}+\mathbf{u}, t+1) = I(\mathbf{x},t)$, hence minimising E_{HS} approximates the brightness constancy assumption.

The root-finding problem formulated in Eq. (5) is easily solved because

$$\nabla_{\mathbf{u}} E_{\mathrm{HS}} = \left(I_t + \mathbf{u}\nabla_{\mathbf{x}} I\right)\nabla_{\mathbf{x}} I, \tag{7}$$

thus introducing the notations $\tilde{\mathbf{g}} = I_t \nabla_{\mathbf{x}} I$ and $\mathbf{H} = H_{\alpha\beta} = I_\alpha I_\beta$, we have

$$\mathbf{g}' = \tilde{\mathbf{g}} + \mathbf{H}\mathbf{u}'. \tag{8}$$

Solving Eq. (5) results in

$$\mathbf{u}' = \mathbf{A}^{-1}\left(\lambda\bar{\mathbf{u}} - \tilde{\mathbf{g}}\right), \tag{9}$$

where $\mathbf{A} = \mathbf{H} + 4\lambda\mathbf{I}$, $\mathbf{I}$ being a unit matrix.

Observe that $\mathbf{A}$ and $\tilde{\mathbf{g}}$ are independent of $\mathbf{u}$ and they can be pre-computed for each image point. This gives a very efficient method [9]. The accuracy can be enhanced by applying a multiscale coarse-to-fine scheme [2], which compensates for the omission of higher-order terms in the Taylor expansion of the brightness constancy equation.

The above scheme can be extended to multiple components I^m using

$$E'_{\mathrm{HS}} = \frac{1}{2}\sum_m \left(I_t^m + \mathbf{u}\nabla_{\mathbf{x}} I^m\right)^2. \tag{10}$$

It can be shown that with $\tilde{\mathbf{g}} = \sum_m I_t^m \nabla_{\mathbf{x}} I^m$ and $\mathbf{H} = \sum_m I_\alpha^m I_\beta^m$ we arrive at the same iterative equations as above.

The image components I^m can be the *RGB* colour channels, the brightness I, the gradients I_x, I_y, or the Laplacian ΔI. One can also go from (R,G,B) to the spherical coordinates and use $(\rho,\ \theta,\ \phi)$ as image components. Combining various components gives a set of different methods [20] that can improve the accuracy of the optical flow [14] and handle changes in illumination [12].

The scheme can be extended to non-linear case [14]. More complex smoothing term [14] and even motion segmentation can be employed [1] to improve the accuracy. (For a recent survey see [20].) In what follows, we present a non-linear scheme which, contrary to the existing methods, makes no assumption on the analytical form of E.

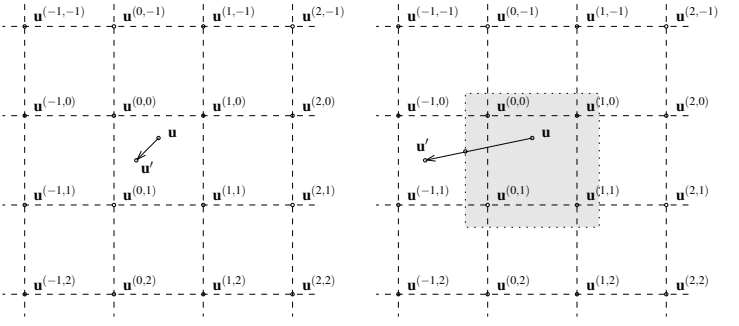

Figure 2: Integer-valued velocity grid and step tolerance.

3 A novel numerical scheme

Our scheme is similar to the Horn-Schunck scheme, however, the root-finding problem formulated in Eq. (5) is solved with Newton's method, while E is calculated only for integer-valued velocities and bicubic interpolation is used to find its first- and second-order derivatives.

For this, we consider $u^{(0,0)} = \lfloor u \rfloor$, $v^{(0,0)} = \lfloor v \rfloor$ and its integer-valued neighbourhood (see Fig. 2)

$$u^{(i,j)} = u^{(0,0)} + i$$
$$v^{(i,j)} = v^{(0,0)} + j,$$

where $i, j \in \{-1, 0, 1, 2\}$.

At given $\mathbf{x}$, we calculate E for $\mathbf{u}^{(i,j)}$ and denote these values by

$$E_{\mathbf{u}}^{(i,j)} = E\left(\mathbf{x}, \mathbf{u}^{(i,j)}\right).$$

The first-order derivatives of E at $\mathbf{u}^{(i,j)}$ can be approximated as

$$E_u \approx \frac{1}{2}\left[E_{\mathbf{u}}^{(i+1,j)} - E_{\mathbf{u}}^{(i-1,j)}\right],$$
$$E_v \approx \frac{1}{2}\left[E_{\mathbf{u}}^{(i,j+1)} - E_{\mathbf{u}}^{(i,j-1)}\right].$$

The cross-derivative is given by

$$E_{uv} \approx \frac{1}{4}\left[E_{\mathbf{u}}^{(i+1,j+1)} - E_{\mathbf{u}}^{(i-1,j+1)} E_{\mathbf{u}}^{(i+1,j-1)} + E_{\mathbf{u}}^{(i-1,j-1)}\right].$$

After computing the above derivatives for all $i, j \in \{0, 1\}$, we can calculate the coefficients C_{kl} of bicubic interpolation[1], which approximates E as

$$E(\mathbf{x}, \mathbf{u}) \approx \sum_{k=0}^{3} \sum_{l=0}^{3} C_{kl} \hat{u}^k \hat{v}^l,$$

[1] Calculating C_{kl} amounts to multiplying a 16×16 constant matrix with a 16 dimensional vector. For details see [16].

where $\hat{\mathbf{u}} = \mathbf{u} - \mathbf{u}^{(0,0)}$. Using this interpolation, we can easily estimate the derivatives of E at any $\mathbf{u}$ in the cell delimited by the velocity points $(0,0)$, $(0,1)$, $(1,0)$, and $(1,1)$. (See Fig. 2.) According to this, the first-order derivatives are

$$E_u \approx \sum_{k=0}^{3}\sum_{l=0}^{3} kC_{kl}\hat{u}^{k-1}\hat{v}^{l},$$
$$E_v \approx \sum_{k=0}^{3}\sum_{l=0}^{3} lC_{kl}\hat{u}^{k}\hat{v}^{l-1},$$

and the second-order derivatives are

$$E_{uu} \approx \sum_{k=0}^{3}\sum_{l=0}^{3} k(k-1)C_{kl}\hat{u}^{k-2}\hat{v}^{l},$$
$$E_{uv} \approx \sum_{k=0}^{3}\sum_{l=0}^{3} l(l-1)C_{kl}\hat{u}^{k}\hat{v}^{l-2},$$
$$E_{vv} \approx \sum_{k=0}^{3}\sum_{l=0}^{3} klC_{kl}\hat{u}^{k-1}\hat{v}^{l-1}.$$

As the bicubic interpolation maintains the continuity of first-order derivatives across cell boundaries, we can solve the non-linear root finding problem given in Eq. (5) with Newton's method.

Introducing the notations $\mathbf{g} = \nabla_{\mathbf{u}} E$ and $\mathbf{H} = E_{\upsilon\nu}$, where $\upsilon, \nu \in \{u, v\}$, we have

$$\mathbf{g}' \approx \mathbf{g} + \mathbf{H}\left(\mathbf{u}' - \mathbf{u}\right),$$

which we plug into Eq. (5) and solve

$$\mathbf{g} + \mathbf{H}\left(\mathbf{u}' - \mathbf{u}\right) - \lambda\left(\bar{\mathbf{u}} - 4\mathbf{u}'\right) = 0.$$

This gives the fixed-point equation

$$\mathbf{u}' = \mathbf{A}^{-1}\left(\lambda\bar{\mathbf{u}} - \mathbf{g} + \mathbf{H}\mathbf{u}\right), \tag{11}$$

where $\mathbf{A} = \mathbf{H} + 4\lambda\mathbf{I}$. With a multiscale approach [2] common to variational optical flow methods, we assure that the iteration starts from a point close to the final solution and thus, if the gradients E_u, E_v are not too large, the iteration either remains in the initial cell or moves smoothly to a neighbouring cell.

If the gradients are too steep, typically for regions where intensity changes cannot be modelled with optical flow, numerical instability may develop. To overcome this, we introduce a step tolerance and clip $\mathbf{u}'$ to the corresponding tolerance region. (See Fig. 2.)

Because the iteration evolves towards a steady state and localises, the value of the step tolerance does not affect the result. It only makes sure that in any problematic point the iteration continues in a neighbouring cell. The 'interaction' with neighbouring pixels (i.e., the smoothness constraint) enforces a solution for any such point.

Observe that $\mathbf{g}$ and $\mathbf{H}$ depend on $\mathbf{u}$ and cannot be pre-computed in this approach. However, they are obtained fast from the bicubic interpolation, which has to be reinitialised only if the iteration moves outside the current cell. When changing to a neighbouring cell, as a further advantage, we do not have to recompute all the 16 $E_{\mathbf{u}}^{(i,j)}$ values, only the 4 new ones.

4 Illumination-robust optical flow

The scheme presented above makes no assumption on the analytical form of the optical constraints. In this section, we present a choice for the data term E that results in an illumination-robust method. For this, we will use cross-correlation in a small window as the metric in E. Recently, a fast, explicit linearised variational flow algorithm based on cross-correlation was proposed [13] and shown to be robust to changes in illumination and visibility. Earlier, a sophisticated non-linear variational framework using different statistical criteria, including cross-correlation, had been applied to elastic image matching [7], motion compensation [19], and 3D scene flow estimation [15].

We consider a sequence of multicomponent images $I^m(\mathbf{x},t)$ and a small pixel neighbourhood $N(\mathbf{x})$. The average pixel value in this block is

$$\bar{I}^m(\mathbf{x},t) = \frac{1}{|N(\mathbf{x})|} \sum_{\mathbf{x}' \in N(\mathbf{x})} I^m(\mathbf{x}',t),$$

and the variance is

$$\sigma_m^2(\mathbf{x},t) = \frac{1}{|N(\mathbf{x})|} \sum_{\mathbf{x}' \in N(\mathbf{x})} \left(I^m(\mathbf{x}',t) - \bar{I}^m(\mathbf{x},t)\right)^2,$$

where $|N(\mathbf{x})|$ is the area of $N(\mathbf{x})$.

In each point $\mathbf{x}$, we take the cross-correlation

$$C_m = \sum_{\mathbf{x}' \in N(\mathbf{x})} \hat{I}^m(\mathbf{x}'+\mathbf{u},t+1)\hat{I}^m(\mathbf{x}',t) \tag{12}$$

of the mean-shifted normalised pixel values

$$\hat{I}^m(\mathbf{x}',t) = \frac{I^m(\mathbf{x}',t) - \bar{I}^m(\mathbf{x},t)}{\sigma_m(\mathbf{x},t)} \tag{13}$$

and define

$$E_{\mathrm{CC}} = \sum_m w_m \left|1 - C_m\right|, \tag{14}$$

where w_m is the weight of the component m. Observe that C_m is invariant to any linear change in I^m. In the next section, we demonstrate by experimental results that E_{CC} used in the numerical scheme presented before leads to an optical flow calculation method which is robust against changes in illumination.

5 Tests and results

To demonstrate the robustness of E_{CC}, we compare the above illumination invariant scheme to the Horn-Schunck method [9] and a method based on our implicit non-linear scheme using the L_1 metric:

$$E_{\mathrm{Diff}} = \sum_m w_m D_m, \tag{15}$$

$$D_m = \frac{1}{|N(\mathbf{x})|} \sum_{\mathbf{x}' \in N(\mathbf{x})} \left|I^m(\mathbf{u}+\mathbf{x}',t+1) - I^m(\mathbf{x}',t)\right|. \tag{16}$$

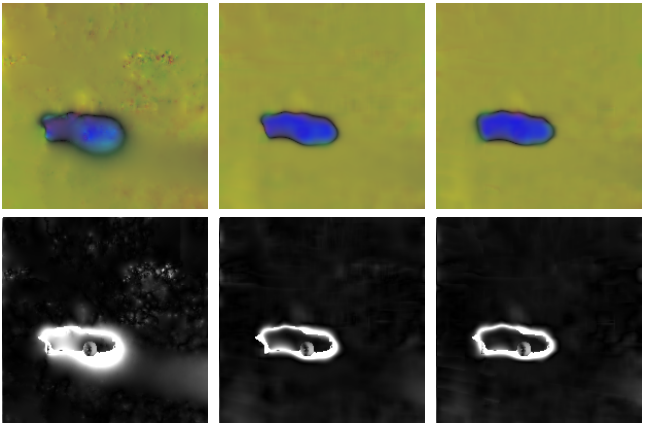

Horn-Schunck $\lambda = 0.03$ | E_{Diff} $\lambda = 0.005$ | E_{CC} $\lambda = 3$

Figure 3: Estimated optical flow and angular error for the original `street` sequence. (See the ground-truth in Fig. 1.)

Notice that E_{Diff} is based on block matching similar to E_{CC}, however, E_{Diff} is not invariant to intensity changes.

The results obtained for the `street` sequence [11] are presented in Fig. 3. We executed 1000 iteration steps on a Gaussian pyramid of 3 levels and scale factor 0.5. The step tolerance was set to 50%. The size of N was 11×11. (The values of λ are given in Fig. 3.)

We compared the computed optical flow to the available ground-truth data [11]. The angular error [3] is calculated as

$$\arccos\left[\frac{u\hat{u}+v\hat{v}+1}{\sqrt{(u^2+v^2+1)(\hat{u}^2+\hat{v}^2+1)}}\right],$$

where $\mathbf{u}$ is the estimated flow, $\hat{\mathbf{u}}$ the ground-truth flow. Fig. 3 shows that both E_{Diff} and E_{CC} perform significantly better than the Horn-Schunck flow.

To test the robustness to illumination changes, we modified the second image of the processed image pair using the transformation

$$I^{m\prime}(\mathbf{x}) = I^m(\mathbf{x})\left[1+1.5\,\xi(\mathbf{x})\right] + 10\,\xi(\mathbf{x}),$$

where $\xi(\mathbf{x}) = \exp\left[-\frac{|\mathbf{x}-\mathbf{x}_0|^2}{5000}\right]$ and $\mathbf{x}_0 = (100,135)$. (See Fig. 4.) The original $I^m(\mathbf{x})$ is an integer in the interval $[0,255]$, and we re-quantised the transformed values to $[0,255]$, too. We will call this artificial illumination change the added effect.

The obtained results are shown in Fig. 5. Both the Horn-Schunck flow and E_{Diff} fail completely to handle these intensity changes. However, the method based on E_{CC} provides an optical flow close to the ground-truth.

We are currently testing the proposed framework for different image sequences, components and metrics. Tab. 1 shows selected comparative results for the `street` sequence. In the table, each pair of numbers gives the average angular error (AAE) without illumination change (left) and with the change (right). The first row presents results obtained using cross-correlation in a small window as defined in Eq. (14). In the second row, the results were

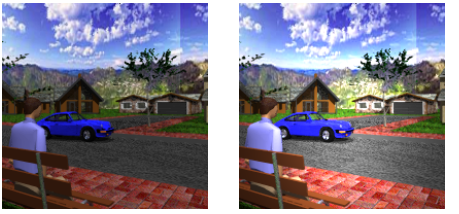

Figure 4: The `street` sequence with illumination change.

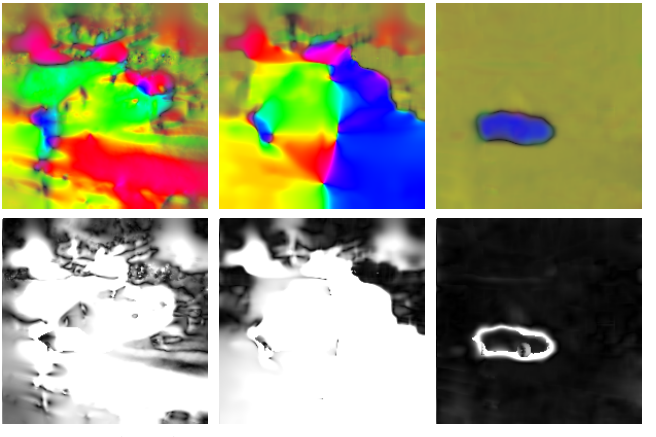

Horn-Schunck E_{Diff} E_{CC}

Figure 5: Estimated optical flow and angular error for the `street` sequence with illumination change. (See Fig. 4.)

obtained using the L_1 metric. For compatibility with the existing point-wise methods, the window size was set to 1. (Recall that the results in Fig. 3 and Fig. 5 were obtained with the window size 11.) In this way, we can mimic different existing algorithms using the proposed implicit scheme. In all cases, the standard smoothness term defined in Eq. (2) was used.

The columns of Tab. 1 represent different combinations of multiple components, that is, colour codes and other images features. In particular, the entry L_1–R,G,B is essentially a colour version of the Horn-Schunck functional [9] using the L_1 metric. As already discussed, the Horn-Schunck algorithm works reasonably well for the original data but fails when the effect is added. The cross-correlation version of the algorithm CC–R,G,B is robust. The robustness of the L_1 variant can be improved by using the spherical representation of colour, ρ,θ,ϕ, as proposed by Mileva et al. [12]; however, the accuracy of L_1–ρ, θ, ϕ is lower than that of CC–R,G,B. (Note that this is *not* an implementation of the algorithm [12], and the added effect is also different.) Another option is to add to the energy term the first and higher order derivatives of the image function, which leads to the variants L_1–R,G,B, I_x,I_y

metric	R,G,B		ρ,θ,ϕ		R,G,B,I_x,I_y		$I,I_x,I_y,\Delta I$	
CC	5.24°	5.20°	5.22°	5.28°	4.23°	4.24°	4.36°	4.34°
L_1	5.00°	16.91°	7.20°	7.87°	4.98°	6.77°	5.05°	5.80°

Table 1: Average angular errors for the `street` images without effect (left number) and with effect (right number) for different multiple components and metrics.

image 1 image 2 image 2 with effect

Figure 6: Two images of the `office` sequence [11] and the second image with illumination change.

metric	R,G,B		ρ,θ,ϕ		R,G,B,I_x,I_y		$I,I_x,I_y,\Delta I$	
CC	9.01°	9.47°	9.68°	9.62°	6.07°	7.66°	5.27°	6.51°
L_1	8.58°	15.67°	9.91°	10.53°	8.62°	10.75°	8.77°	7.88°

Table 2: Average angular errors for the `office` images without effect (left number) and with effect (right number) for different multiple components and metrics.

and L_1–$I,I_x,I_y,\Delta I$ that are similar in spirit to modern precise algorithms like [4]. Observe, however, that cross-correlation yields higher precision in all cases except for the effect-free R,G,B where L_1 is slightly better.

Tab. 2 shows similar comparative results for the `office` sequence [11] illustrated in Fig. 6. The same artificial illumination change has been added to the first image to test the robustness of the different metrics and combinations of multiple components. The errors are, generally, somewhat larger, but the main trends are the same as for the `street` sequence. In particular, cross-correlation again provides robistness and improves precision in almost all cases, while the most precise method for the `office` sequence is the greyscale algorithm CC–$I,I_x,I_y,\Delta I$. This means that cross-correlation based optical flow can handle illumination changes in greyscale sequences, while the method [12] is only applicable to colour data.

6 Conclusion

We presented an implicit non-linear numerical scheme for optical flow calculation based on the variational approach and proposed a non-linear optical constraint robust against changes in illumination. The presented optical constraint is formulated as block-matching based on normalised cross-correlation.

The algorithmic complexity of the scheme depends only slightly on the block size, because the optical constraints are evaluated on-demand only for integer-valued velocities. The presented iterative solver uses a bicubic interpolation over this discrete velocities. The iterative process, when close to the steady state, localises and thus recalculating the interpolation is not needed over a large number of steps.

Preliminary results show that the scheme can outperform some traditional methods, it can produce high accuracy optical flow, and works for both single and multicomponent images. In particular, optical constraint with normalised cross-correlation is robust to illumination changes in greyscale data when the approach [12] based on the photometric invariants of the dichromatic reflection model [17] is not applicable.

A more comprehensive evaluation is in progress. Further research should also investigate

the possibility of using other illumination invariant optical constraints and the applicability of the method to real-world motion estimation problems.

Acknowledgements

This research was supported in part by the NKTH-OTKA grant CK 78409 and by the Network of Excellence MUSCLE (FP6-507752).

References

[1] T. Amiaz and N. Kiryati. Piecewise-smooth dense optical flow via level sets. *International Journal of Computer Vision*, 68:111–124, 2006.

[2] P. Anandan. A computational framework and an algorithm for the measurement of visual motion. *International Journal of Computer Vision*, 2:283–310, 1989.

[3] J. L. Barron, D. J. Fleet, and S. S. Beauchemin. Performance of optical flow techniques. *International Journal of Computer Vision*, 12:43–77, 1994.

[4] T. Brox, A. Bruhn, N. Papenberg, and J. Weickert. High accuracy optical flow estimation based on a theory for warping. In *Proc. European Conf. on Computer Vision*, volume IV, pages 25–36, 2004.

[5] V. I. Bruce, P. R. Green, and M. Georgeson. *Visual Perception*. Psychology Press (UK), 1996.

[6] J. Gibson. *The Senses Considered as Perceptual Systems*. Houghton Mifflin – Boston, 1966.

[7] G. Hermosillo, C. Chefd'hotel, and O. Faugeras. Variational Methods for Multimodal Image Matching. *International Journal of Computer Vision*, 50:329–343, 2002.

[8] B. K. P. Horn. *Robot Vision*. McGraw-Hill – New York, 1986.

[9] B. K. P. Horn and B. G. Schunck. Determining optical flow. *Artificial Intelligence*, 17: 185–203, 1981.

[10] B. D. Lucas and T. Kanade. An iterative image registration technique with an application to stereo vision. In *DARPA Image Understanding Workshop*, pages 121–130, 1981.

[11] B. McCane, K. Novins, D. Crannitch, and B. Galvin. On Benchmarking Optical Flow. *Computer Vision and Image Understanding*, 84:126–142, 2001.

[12] Y. Mileva, A. Bruhn, and J. Weickert. Illumination-robust variational optical flow with photometric invariants. In *DAGM-Symposium*, pages 152–162, 2007.

[13] J. Molnár and D. Chetverikov. Illumination-robust variational optical flow based on cross-correlation. In 33rd *Workshop of the Austrian Association for Pattern Recognition*, pages 119–128, May 2009.

[14] N. Papenberg, A. Bruhn, T. Brox, S. Didas, and J. Weickert. Highly accurate optic flow computation with theoretically justified warping. *International Journal of Computer Vision*, 67:141–158, 2006.

[15] J.-P. Pons, R. Keriven, O. Faugerasand, and G. Hermosillo. Variational Stereovision and 3D Scene Flow Estimation with Statistical Similarity Measures. In *Proc. International Conf. on Computer Vision*, volume 1, pages 597–602, 2003.

[16] W. Press, S. Teukolsky, W. Vetterling, and B. Flannery. *Numerical Recipes in C*. Cambridge University Press, Cambridge, UK, 2nd edition, 1992.

[17] S.A. Shafer. Using color to separate reflection components. *Color Research and Applications*, 10(4):210–218, 1985.

[18] D. Todorovic. A gem from the past: Pleikart Stumpf's anticipation of the aperture problem, Reichardt detectors, and perceived motion loss at equiluminance. *Perception*, 25:1235–1242, 1996.

[19] G. Hermosillo Valadez. Method and System for Motion Compensation in a Temporal Sequence of Images. US Patent Application Publication, 2005. Pub. No.: US 2005/0265611 A1.

[20] J. Weickert, A. Bruhn, T. Brox, and N. Papenberg. *Mathematical Models for Registration and Applications to Medical Imaging*, volume 10 of *Mathematics in Industry*, chapter A Survey on Variational Optic Flow Methods for Small Displacements, pages 103–136. Springer Berlin Heidelberg, 2006.